

## Comparing cyclohexyl hydroxamic acid and benzohydroxamic acid in cassiterite flotation under lead nitrate activation

Hao Yang, Leming Ou

School of Minerals Processing and Bioengineering, Central South University, Changsha 410083, China

Corresponding author: [olm@csu.edu.cn](mailto:olm@csu.edu.cn) (Leming Ou)

**Abstract:** This paper investigates the flotation behavior of Cyclohexyl hydroxamic acid (CHA) and benzhydroxamic acid (BHA) on cassiterite under lead nitrate activation conditions and elucidates the adsorption mechanism of CHA on the cassiterite surface. Microflotation experiments were performed to compare the capturing efficiency of CHA and BHA at pH values ranging from 4 to 12. Results showed that CHA exhibited superior capability in capturing cassiterite compared to BHA. The recovery of cassiterite in the hydroxamic acid-based flotation system correlated positively with the adsorption of hydroxamic acid on the cassiterite surface. Adsorption experiments revealed an increase in adsorption quantity with an increase in hydroxamic acid dosage, with CHA exhibiting significantly higher adsorption amount than BHA on the cassiterite surface. To analyze the adsorption mechanism of CHA on the cassiterite surface, both infrared spectroscopy and X-ray photoelectron spectroscopy (XPS) analysis were conducted, both before and after lead nitrate activation. IR spectra and XPS results indicated that lead ion activation enhanced the adsorption of CHA on the cassiterite surface, resulting in an increased number of active sites for CHA interaction. Additionally, chemisorption of CHA occurred on the cassiterite surface.

**Keywords:** adsorption, cassiterite, flotation, lead nitrate, cyclohexyl hydroxamic acid

### 1. Introduction

Tin (Sn, Stannum) is a metallic element characterized by a silvery-white luster. It was among the earliest metals discovered and utilized by humankind. Its notable features include a low melting point, soft texture, high plasticity, corrosion resistance, and ease of alloy formation (Schneider et al., 2023). Consequently, tin finds widespread application in the manufacturing and production of solder, tin-plated plates (Pandey et al., 2023), alloys, float glass, and various other products (Jin and Ou, 2021). The high density of cassiterite necessitates re-election as the primary method for its extraction. However, during the grinding process, cassiterite is prone to over-crushing due to its brittle nature (Angadi et al., 2015). Furthermore, achieving recovery objectives for the microfine fraction of cassiterite through re-election poses significant challenges. Therefore, flotation serves as the principal technique for recovering microfine cassiterite (Leistner et al., 2016; Wang et al., 2013; Zhou et al., 2014).

The selection of appropriate collectors is a crucial factor influencing the flotation recovery of cassiterite. Currently, the commonly used cassiterite collectors in industry include fatty acids, arsenic acids, alkyl hydroxycarboxylic acids, alkyl sulfosuccinic acids, and phosphonic acids (Feng et al., 2018; Li et al., 2015; Qin et al., 2011; Zhu et al., 2022). Among these, fatty acids primarily feature the carboxyl group as their main functional group, which enables easy synthesis, low cost, and strong collecting ability. Oleic acid, an early fatty acid collector, demonstrates optimal flotation performance under neutral or weak alkaline conditions (Jin and Ou, 2022). Xu and Qin (Xu and Qin, 2012) investigated the mechanism of sodium oleate on cassiterite and observed that the free energy of sodium oleate adsorption on the cassiterite surface reached 8.36 kcal/mol at pH 7.8, coinciding with the maximum adsorption capacity and cassiterite flotation recovery. Nevertheless, sodium oleate exhibits poor selectivity and susceptibility to interference from Ca and Mg ions in the pulp solution. Phosphonic acid-based collectors can be categorized into aromatic phosphonic acids and aliphatic phosphonic acids (Gruner and Bilsing, 1992). These agents possess low toxicity and exhibit excellent collecting

performance, rendering them potential substitutes for arsenical acid agents. The adsorption mechanism of  $\alpha$ -hydroxyoctyl phosphonic acid on the cassiterite surface has been documented. In comparison with styrene phosphonic acid, bisphosphonic acid, benzyl hydroxamic acid, and salicyl hydroxamic acid,  $\alpha$ -hydroxyoctyl phosphonic acid demonstrates a superior collecting effect on cassiterite, albeit with reduced selectivity (Li et al., 2015). The presence of  $\text{Ca}^{2+}$  and  $\text{Fe}^{2+}$  generated through mineral dissolution interferes with the collecting efficacy of phosphonic acid. Conversely, short-chain hydroxamic acid-based collectors exhibit enhanced selectivity and low toxicity for cassiterite. The robust chelating ability of hydroxamic acid with metal ions arises from its molecular structure, wherein the oxygen and nitrogen atoms serve as ligands for forming various metal ion complexes. Hydroxamic acid is characterized by the functional group  $-\text{CONHOH}$ , which typically exhibits two interchangeable isomers, ketone and alcohol, with the molecular formulas  $\text{R}-\text{C}(=\text{O})-\text{NHOH}$  and  $\text{R}-\text{COH}(=\text{N})-\text{OH}$ . The R group may consist of a hydrocarbon or aromatic group (Zhao et al., 2013). Common aromatic hydroxamic acids include benzyl hydroxamic acid and salicyl hydroxamic acid. Benzyl hydroxamic acid functions as a collector for the selective separation of cassiterite, calcite, and quartz, displaying robust collecting capability for cassiterite while exerting minimal effect on quartz. Kinetic potential and infrared spectroscopy analyses confirmed the chemisorption of benzyl hydroxamic acid onto the surface of cassiterite (Wu and Zhu, 2006). Salicyl hydroxamic acid proved effective as a collector for cassiterite, forming chelates on the cassiterite surface under neutral conditions. Adsorption amount tests substantiated the maximum adsorption capacity of salicyl hydroxamic acid at pH 6.5, coinciding with the peak cassiterite recovery rate (Qin et al., 2012; Qin et al., 2011).

Studies have revealed that the effective recovery of cassiterite cannot be achieved solely through the use of a single hydroxamic acid or its increased dosage. This limitation arises from the inherent difficulty of the cassiterite surface to provide an ample number of adsorption sites for hydroxamic acids, indicating a scarcity of active binding sites (Chen, 2021; Chen and Li, 2022). To surmount this obstacle, an artificial introduction of specific metal ions onto the cassiterite surface is often employed to augment the availability of active reaction sites between the reagents and the mineral, thereby enhancing the overall efficacy of the process (Feng et al., 2016; Sarvaramini et al., 2016; Zhao et al., 2015). In the pulp system, a variety of metal ions, including  $\text{Pb}^{2+}$ ,  $\text{Fe}^{3+}$ ,  $\text{Zn}^{2+}$ ,  $\text{Ca}^{2+}$ ,  $\text{Mg}^{2+}$ , etc., may be present, and all of these ions can influence the interaction process between the collector and the mineral (Ruan et al., 2018; Xie et al., 2021).  $\text{Pb}^{2+}$  commonly acts as an activator for cassiterite in the benzohydroxamic acid flotation system. The effect of  $\text{Pb}^{2+}$  on cassiterite and calcite in mixed mineral systems has been explored using BHA as a collector and CMC as an inhibitor. After the addition of  $\text{Pb}^{2+}$ , the surface potential of cassiterite increased more than that of calcite. This promotes the adsorption of BHA on the surface of cassiterite, which improves the flotation efficiency of cassiterite and solves the difficulty of separating cassiterite and calcite (Tian et al., 2017). One research result revealed that the adsorption of Pb ions on cassiterite surface is facilitated by an intricate interaction between the oxygen vacancies inherent on the surface of cassiterite and the presence of Pb. This intricate interaction not only increases the number of available active sites on the mineral surface, but also contributes to the enhancement of collector adhesion (Feng et al., 2017).

The Cyclohexyl hydroxamic acid (CHA) utilized in this study is derived from the "isomerization" principle of flotation chemicals. By substituting the phenyl group in benzylhydroxamic acid with a cyclohexyl group, the two hydroxamic acids possess similar structures and functional groups. Hence, it is hypothesized that they exhibit comparable capture performance for cassiterite. Consequently, an investigation into the flotation behavior and adsorption mechanism of Cyclohexyl hydroxamic acid on cassiterite becomes imperative. This paper examines and compares the capture efficiency of Cyclohexyl hydroxamic acid and benzylhydroxamic acid on cassiterite under the activation conditions of lead nitrate. Furthermore, the adsorption mechanism of Cyclohexyl hydroxamic acid on the surface of cassiterite is explored through single mineral flotation experiments, adsorption amount tests, infrared spectroscopy analysis, and X-ray photoelectron spectroscopy (XPS) analysis.

## 2. Materials and methods

### 2.1. Materials and chemicals

The cassiterite mineral employed in this experiment was sourced from Yunnan Province, China. Fig. 1 illustrates the X-ray diffraction (XRD) pattern obtained from the diffraction data, confirming the high

purity of cassiterite without any discernible impurities, thus satisfying the experimental prerequisites. The sample was subjected to grinding in a laboratory porcelain mill to produce a particle size product ranging from  $-74 \mu\text{m}$  to  $+38 \mu\text{m}$ , specifically tailored for the flotation experiments. Benzylhydroxamic acid (BHA) and Cyclohexyl hydroxamic acid (CHA) were procured from a pharmaceutical factory located in Hubei Province, with a purity exceeding 99%. Cyclohexyl hydroxamic acid, a novel hydroxamic acid, was synthesized through the hydroxylation reaction involving methyl cyclohexanecarboxylate and hydroxylamine hydrochloride as raw materials, while methanol and water were employed as solvents. Notably, Cyclohexyl hydroxamic acid exhibits superior foaming properties compared to benzylhydroxamic acid. Analytically pure lead nitrate and hydrochloric acid were used for adjusting the pH in the flotation experiments. Furthermore, the hydrochloric acid and sodium hydroxide employed for pH adjustment and lead nitrate, respectively, were of analytical purity. Deionized water with a resistivity exceeding  $18 \text{ M}\Omega \times \text{cm}$  was utilized throughout the entirety of the experiment.

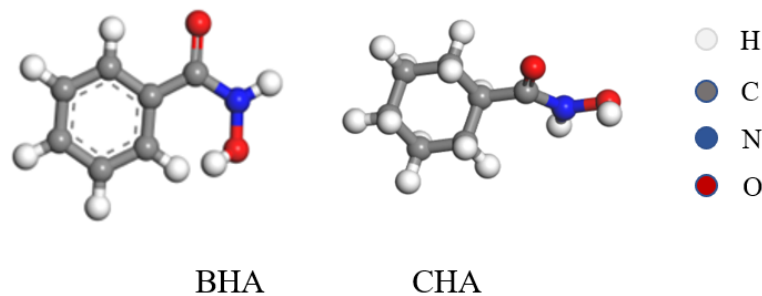


Fig. 1. Ball-and-stick modeling of the molecular structures of BHA and CHA

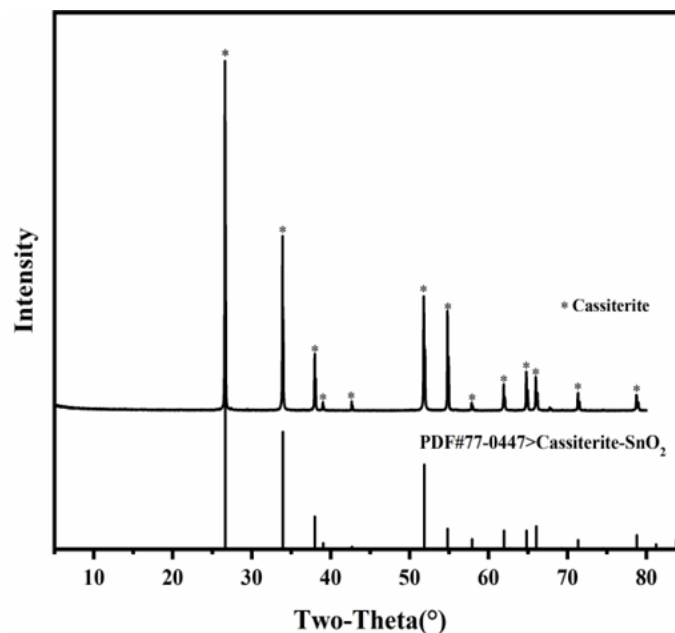


Fig. 2. XRD spectra of the cassiterite

## 2.2. Methods

### 2.2.1. Micro-flotation tests

The flotation experiments were conducted using a 40 mL XFG type hanging tank flotation machine, operating at a fixed speed of 1992 r/min. For each experiment, 2.0 g of ore was precisely weighed and placed into the flotation tank. Subsequently, 38 mL of deionized water was added to the mineral using a measuring cylinder, and the mixture was stirred for 1 minute. Following that, a specific amount of lead nitrate was introduced to activate the system for 3 minutes. After the activation step, a pH adjuster was added and stirred for 3 minutes, while the pH was measured using a PHS-3C precision pH meter. Once the pH measurement was obtained, the trap was added to the system and stirred for 3 minutes,

and flotation was carried out for an additional 3 minutes. The resulting froth products and tailings were filtered, dried, and weighed, allowing for the calculation of cassiterite recovery under each experimental condition. Each test was repeated three times, and then the average of the flotation test recoveries was calculated.

### 2.2.2. Adsorption experiments

The amount of adsorbed trap on the surface of cassiterite was determined using a Shimadzu Total Organic Carbon Analyzer (TOC-VCPH), Japan. For each measurement, 0.5 g of ore was accurately weighed and the dosing sequence and dose corresponding to the flotation experiment was stirred at a constant temperature of 25°C. Subsequently, the suspension was filtered into a centrifuge tube and centrifuged at 9000 rpm for 20 minutes to achieve solid-liquid separation. Once separation was achieved, 25 mL of supernatant was withdrawn into a colorimetric tube for TOC sampling and measurement. The experiment was repeated three times and the mean and standard deviation of the adsorbed amount of collector on cassiterite was calculated based on the TOC value measured each time.

### 2.2.3. FTIR measurements

The samples were finely ground to a particle size of 2  $\mu\text{m}$  using an agate mortar. A beaker was then used to hold 0.5 g of the mineral sample. Following the same sequence as the single mineral flotation test, the collector was added to the beaker to obtain a mixed solution. The solution was stirred with a magnetic stirrer for 20 minutes. After the stirring process, the suspension was centrifuged to obtain a precipitate, which was subsequently rinsed three times with deionized water. The rinsed precipitate was then dried in a vacuum constant temperature oven at 40°C. The dried samples were subjected to Fourier transform infrared (FTIR) spectroscopy using the potassium bromide pressure method. The FTIR analysis was performed on a Nicolet FTIR-740 spectrometer from Thermo, USA, with wave numbers ranging from 400 to 4000  $\text{cm}^{-1}$ . The infrared spectroscopy measurements were conducted immediately after the drying of the pharmaceuticals and grinding of the pure minerals.

### 2.2.4. XPS measurements

The sample preparation process for this experiment was identical to that used for single mineral flotation. Following centrifugation of the conditioned slurry mixture, the resulting precipitate was rinsed three times with deionized water. It was then filtered and dried in a vacuum oven with a constant temperature set at 40°C. Finally, the dried samples were stored under vacuum conditions for testing. X-ray photoelectron spectroscopy (XPS) analysis was conducted using a Thermo Fisher Scientific K-Alpha 1063XPS spectrometer. Data processing was performed using Thermo Scientific Advantage software.

## 3. Results and discussion

### 3.1. Micro-flotation results of cassiterite single minerals

Fig. 3 illustrates the impact of different pH conditions on the flotation recovery of cassiterite with a dosage of 100 mg/L for both BHA and CHA, and a dosage of 40 mg/L for Pb(II). Throughout the entire pH range tested, CHA exhibited significantly superior cassiterite capture ability compared to BHA. Within the pH range of 4-9, the flotation recovery of cassiterite increased for both collectors as the pH increased. However, the maximum increase in cassiterite flotation recovery was observed in the CHA flotation system, reaching 92.53%, which was 17.53 percentage points higher than the recovery achieved in the BHA flotation system. It is worth noting that the cassiterite recoveries showed a declining trend when pH exceeded 9. These findings indicate that, under the condition of fixed dosages of hydroxamic acid and Pb(II), CHA combined with Pb(II) demonstrates a stronger ability to capture cassiterite compared to BHA.

In Fig. 4, the recovery ability of cassiterite was compared at pH=9 and a Pb(II) dosage of 40 mg/L using different amounts of CHA and BHA. As the dosage of hydroxamic acid increased, the recovery of cassiterite increased in both hydroxamic acid flotation systems. When the hydroxamic acid dosage was increased from 20 mg/L to 100 mg/L, the flotation recovery of cassiterite increased from 10.22% to 92.53% when CHA was used as the collector, whereas it increased only from 5.31% to 75% when BHA

was used as the collector. Between the hydroxamic acid dosages of 100 mg/L and 140 mg/L, the recovery of cassiterite remained relatively constant. Throughout the entire range of hydroxamic acid dosage, the flotation recovery of cassiterite was consistently higher with CHA as the collector compared to BHA. These results clearly demonstrate that the combination of CHA with Pb(II) exhibits a stronger ability to capture cassiterite than BHA does.

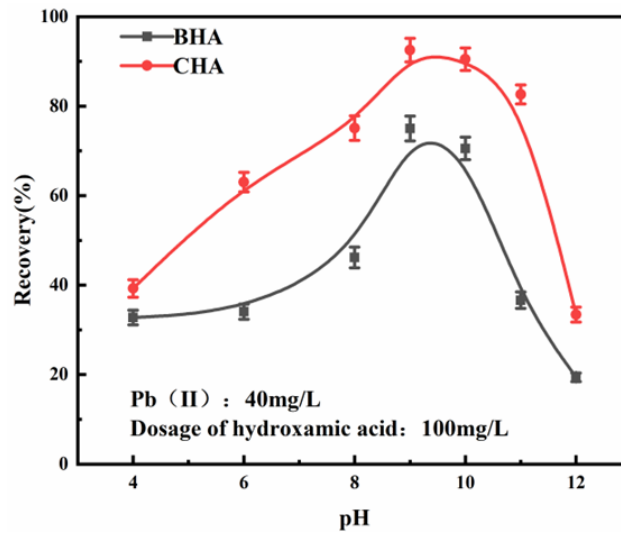


Fig. 3. Effect of pulp pH on cassiterite floatability at hydroxamic acid dosage of 100 mg/L and a Pb(II) dosage of 40 mg/L

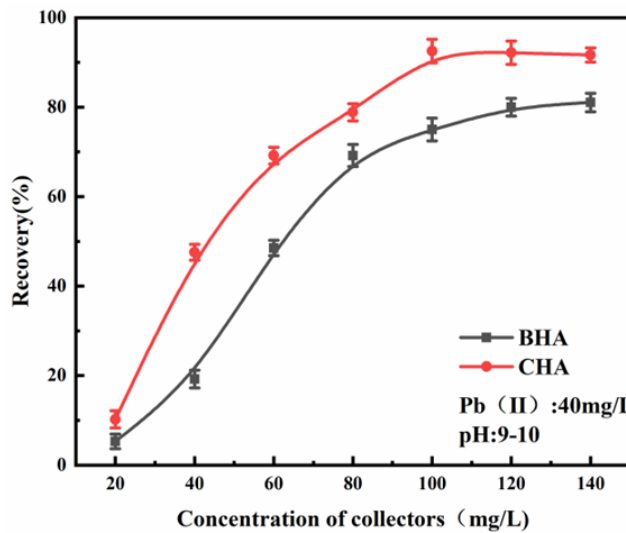


Fig. 4. The effect of hydroxamic acid dosage on the floatability of cassiterite at pH between 9 and 10 and Pb(II) dosage of 40 mg/L

### 3.2. Adsorption experiments

The adsorption of flotation chemicals on the surface of cassiterite is often directly proportional to the cassiterite flotation recovery. To examine the effect of the two hydroxamic acids on cassiterite flotation, the adsorption amount of the hydroxamic acids on the cassiterite surface was investigated at different dosages within the pH range of 9 to 10 and a Pb(II) concentration of 40 mg/L. The relationship between the adsorption amounts of the hydroxamic acids on the cassiterite surface and their initial concentrations is illustrated in Fig. 5. The adsorption amounts of both hydroxamic acids on the surface of cassiterite aligned with the flotation performance. It is evident that the adsorption of both hydroxamic acids on cassiterite increases with the rise in the initial concentration of the agents. Once the dosage of the agents reached 100 mg/L, the rate of increase in the adsorption amount slowed down, which correlates with the flotation results. Although an increase in the initial concentration of both agents led

to greater adsorption on the surface of cassiterite, the adsorption of CHA was higher compared to BHA. This outcome indicates that Cyclohexyl hydroxamic acid possesses a stronger ability to capture cassiterite than benzylhydroxamic acid.

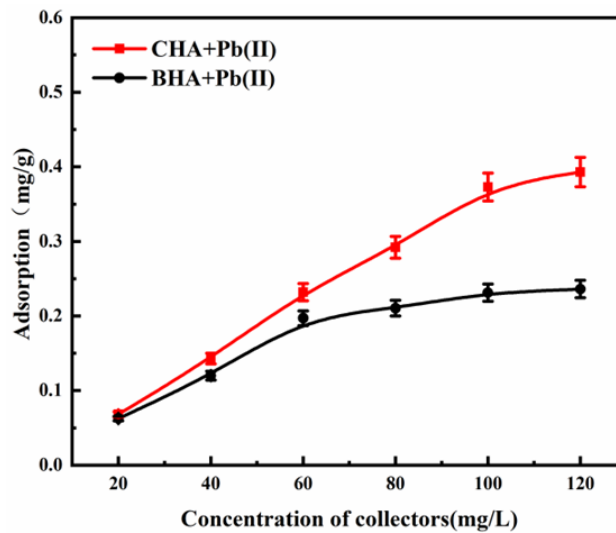


Fig. 5. The relationship between the amount of hydroxamic acid and the amount of hydroxamic acid adsorbed on the surface of cassiterite when the amount of Pb(II) was 40 mg/L

### 3.3. FTIR studies

IR spectroscopy can provide further insights into the adsorption mechanism and collecting effect of Cyclohexyl hydroxamic acid on the surface of cassiterite. Fig. 6 presents the infrared spectra of Cyclohexyl hydroxamic acid, cassiterite treated with Cyclohexyl hydroxamic acid, and cassiterite treated with Cyclohexyl hydroxamic acid and lead ions. In curve a, the IR spectrum of Cyclohexyl hydroxamic acid reveals absorption peaks at 3179.3 cm<sup>-1</sup>, resulting from the overlapping N-H and O-H stretching vibrations, as well as a stretching vibration peak of the N-H group at 3041.31 cm<sup>-1</sup>. The C-H stretching vibration peaks appear at 2925.93 and 2853.89 cm<sup>-1</sup>, while the carbonyl stretching vibration peak of the C=O group is observed at 1545.15 cm<sup>-1</sup>. Additionally, three absorption peaks related to N-O vibrational splitting are observed at 1142.18, 1060.75, and 1022.46 cm<sup>-1</sup> (Huang et al., 2013).

Curve b illustrates the IR spectrum of cassiterite treated with Cyclohexyl hydroxamic acid, where more pronounced absorption peaks appear at approximately 2925.93 and 2853.89 cm<sup>-1</sup>, corresponding to the C-H stretching vibrations in the cycloalkyl group. Notably, the N-H and O-H stretching vibration peaks at 3179.3 cm<sup>-1</sup> and the N-H group at 3041.31 cm<sup>-1</sup> of Cyclohexyl hydroxamic acid nearly disappear upon the addition of CHA.

Curve c displays the IR spectrum of cassiterite treated with lead nitrate followed by Cyclohexyl hydroxamic acid, which closely resembles curve b. The absorption peaks at 2931.40 and 2858.36 cm<sup>-1</sup> correspond to C-H stretching vibrations, exhibiting higher intensities than those observed in curve b. Similar to curve b, the N-H and O-H stretching vibration peaks of Cyclohexyl hydroxamic acid at 3179.3 cm<sup>-1</sup> and 3041.31 cm<sup>-1</sup> are significantly diminished. This indicates that lead nitrate enhances the adsorption of Cyclohexyl hydroxamic acid on the surface of cassiterite and serves as an effective activator for the flotation collecting of cassiterite using Cyclohexyl hydroxamic acid.

### 3.4. XPS spectroscopic analyses

XPS (X-ray photoelectron spectroscopy) is a valuable analytical technique for determining the elemental composition and chemical states of mineral surfaces (Ocelli and Stencil, 1987). Fig. 7 displays the XPS spectra of untreated and treated cassiterite surfaces using flotation chemicals. In Fig. 7(a), the XPS spectrum of the cassiterite surface treated with deionized water shows no impurities other than the carbon peak, confirming the high purity of the cassiterite sample. Fig. 7(b) exhibits the spectrum of the cassiterite surface treated with lead nitrate, where the presence of the characteristic Pb4f peak confirms the adsorption of Pb(II) on the cassiterite surface. Fig. 7(c) illustrates the XPS spectrum of the cassiterite

surface treated with Cyclohexyl hydroxamic acid (CHA). A weak new peak near 400 eV suggests that a small amount of CHA is adsorbed onto the inert cassiterite surface. Fig. 7(d) demonstrates the surface spectra of cassiterite treated with both lead nitrate and CHA. Here, the intensity of the N1s spectrum is stronger compared to that of cassiterite treated with CHA alone. Overall, XPS analysis provides valuable information on the elemental composition and chemical states of the cassiterite surface, confirming the adsorption of lead ions and hydroxamic acid on the cassiterite surface during the flotation process.

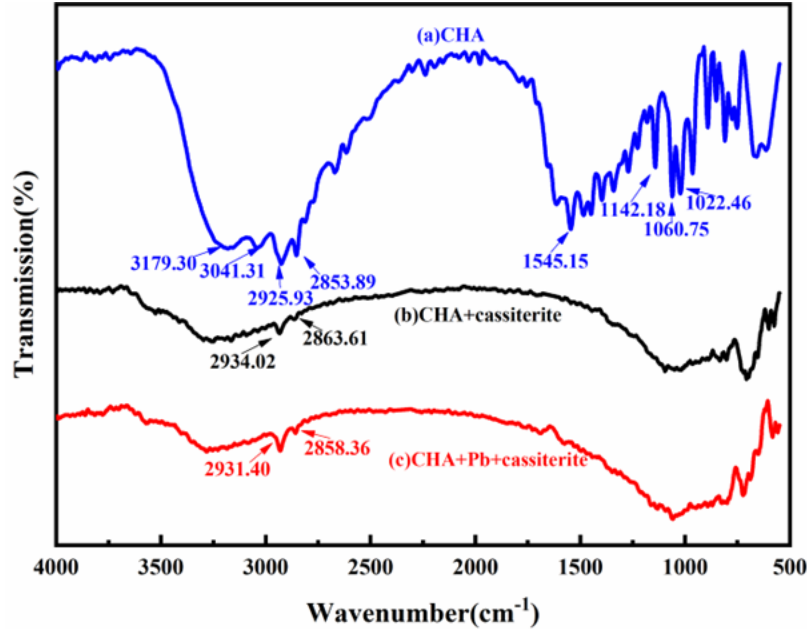


Fig. 6. FTIR spectra of cassiterite before and after treatment with flotation chemicals

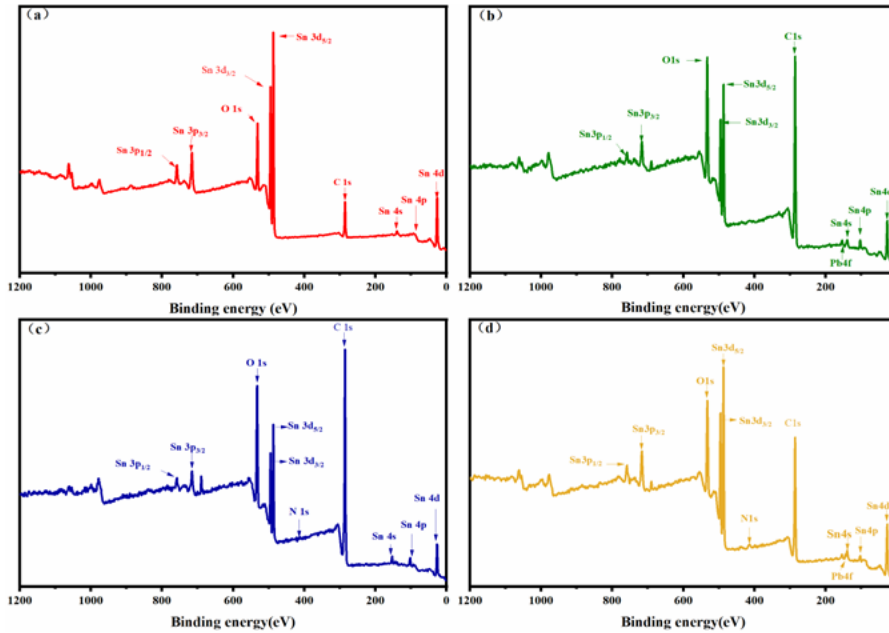


Fig. 7. XPS spectra of cassiterite surface after treated with (a) denionized water, (b) Pb(II), (c) CHA and (d) both Pb(II) and CHA

In Table 1, the relative atomic concentrations of C, O, Sn, N, and Pb on the cassiterite surface are presented after treatment with different chemical systems. The relative concentrations of each atom on the cassiterite surface treated with Pb(II) only were found to be similar to those on the untreated cassiterite surface. This suggests that Pb(II) alone did not significantly impact the atomic composition of the cassiterite surface. When comparing the cassiterite surface treated with CHA only to the surface activated by adding Pb(II) and subsequently treated with CHA, there was an increase of 4.92% in the

relative concentration of C and a 0.38% increase in the relative concentration of N. This indicates that the addition of Pb(II) to the system contributed to the adsorption of CHA on the cassiterite surface. Overall, these results suggest that the presence of Pb(II) enhances the adsorption of CHA onto the cassiterite surface, as evidenced by the observed changes in relative atomic concentrations.

Table 1. Relative atomic concentration of the main elements on the surface of cassiterite.

Samples	Atomic concentration (%)				
	C	O	Sn	N	Pb
Without flotation reagents treatment	53.67	28.09	18.24	–	–
After CHA treatment	65.7	25.99	7.58	0.73	–
After lead nitrate treatment	58.41	22.74	18.63	–	0.22
In the presence of lead nitrate and CHA	70.62	21.5	6.4	1.11	0.37

Fig. 8: Sn 3d Narrow Scan XPS Photoelectron Spectra of Cassiterite Treated with Different Flotation Agents. In Fig. 8, the Sn 3d narrow scan XPS photoelectron spectra of cassiterite particles treated with different flotation agents are presented, providing insights into the interactions between the agents and the cassiterite surface. Fig. 8(a) displays the XPS spectrum of the cassiterite sample after deionized water treatment. The binding energies of 486.62 eV and 495.02 eV for Sn 3d<sub>5/2</sub> and Sn 3d<sub>3/2</sub>, respectively, are assigned to Sn<sup>4+</sup> on the SnO<sub>2</sub> lattice surface (Sukunta et al., 2017; Sun et al., 2020). This indicates the presence of Sn<sup>4+</sup> species on the surface of cassiterite in its pristine state. Fig. 8(b) exhibits the XPS spectra of CHA-treated cassiterite samples. The Sn 3d<sub>5/2</sub> and Sn 3d<sub>3/2</sub> spectra show only slight changes compared to those of cassiterite without the addition of a flotation agent. This suggests weak adsorption of CHA by the Sn sites on the cassiterite surface. The Sn atoms seem to have limited interaction with CHA, resulting in minimal alteration of the Sn 3d binding energies. Fig. 8(c) showcases the XPS spectra of cassiterite treated with lead nitrate. The Sn 3d<sub>5/2</sub> and Sn 3d<sub>3/2</sub> peaks are located at 486.52 eV and 494.91 eV, respectively. The binding energies are similar to those observed in pure cassiterite, indicating that Pb(II) and its hydroxide species are not directly involved in the reaction of Sn atoms on the surface of cassiterite. The presence of lead nitrate does not induce significant changes in the Sn 3d binding energies. Fig. 8(d) presents the surface spectra of cassiterite treated with Pb(II) and CHA. The binding energy of the Sn 3d peak remains relatively unchanged compared to the untreated cassiterite,

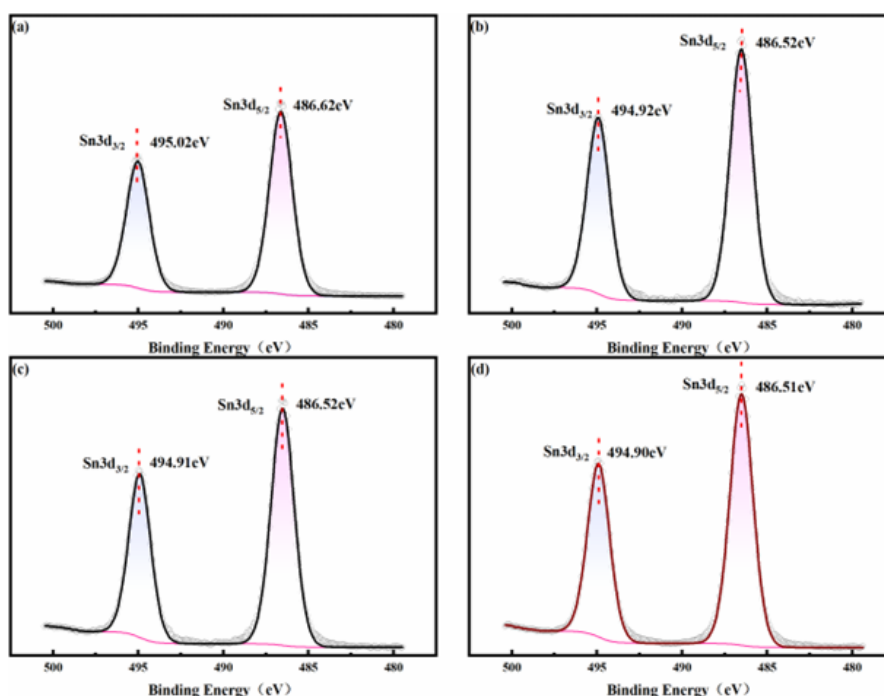


Fig. 8. XPS narrow-scan spectra of Sn 3d on the cassiterite surface after being treated with (a) deionized water, (b) CHA, (c) Pb (II) and (d) both Pb(II) and CHA

suggesting that the interaction between CHA and Sn atoms on the cassiterite surface does not cause substantial shifts in the Sn 3d binding energies. These findings imply that the Sn atoms on the mineral surface are temporarily engaged in the adsorption process involving Pb(II) and CHA. In summary, the Sn 3d XPS spectra provide evidence of the weak adsorption of CHA by Sn sites on the cassiterite surface and suggest that the Sn atoms are temporarily involved in the adsorption of Pb(II) in conjunction with CHA.

Fig. 9 depicts the XPS spectra of the deionized water-treated cassiterite sample and the cassiterite sample treated with a flotation agent, specifically focusing on the O 1s region. In Fig. 9(a), the XPS spectrum of the pure cassiterite sample reveals three distinct peaks located at binding energies of 530.53 eV, 532.01 eV, and 533.13 eV. According to literature, these peaks can be attributed to the cassiterite native oxide (O3), the bridging oxygen atoms on the cassiterite surface (Obri), and the hydroxylated cassiterite surface resulting from water molecule adsorption on the cassiterite surface (Snsurf-OH, Oterm) (Cao et al., 2021; Machesky et al., 2011; Tian et al., 2018). Given the shared crystal structure between rutile and cassiterite, the observed O 1s photoelectron spectrum is consistent with the O1s spectrum of rutile. Fig. 9(b) displays the XPS spectra of the cassiterite surface treated with CHA, revealing insignificant shifts in the aforementioned peaks. This observation suggests the challenging adsorption of the flotation agent CHA onto the cassiterite surface in the absence of Pb(II) activation. In Fig. 9(c), the XPS spectra of the cassiterite surface modified by Pb(II) treatment followed by CHA treatment are presented. Notably, the corresponding bridged Obri atoms and hydroxylated Oterm atoms on the cassiterite surface exhibit upward shifts in binding energies, with increases of 0.05 eV and 0.22 eV, respectively, compared to those in Fig. 9(b). This shift indicates that CHA adsorption on the modified cassiterite surface induces alterations in the chemical environment of oxygen atoms. The upward shift in the oxygen 1s XPS peak is attributed to a decrease in electron cloud density.

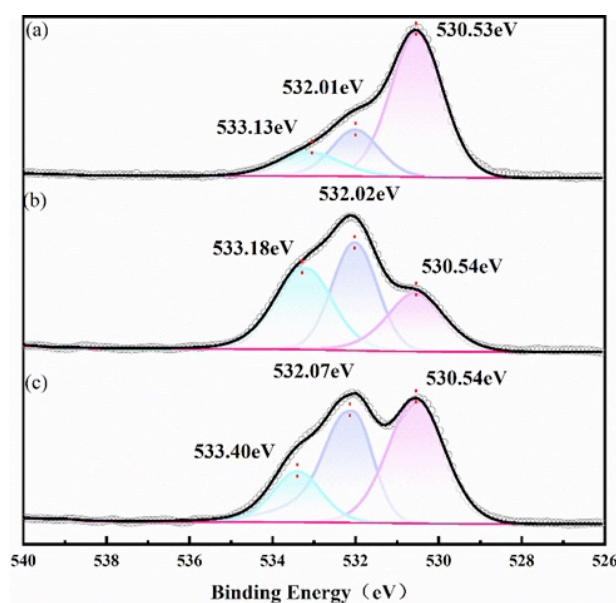


Fig. 9. XPS narrow-scan spectra of O 1s on the cassiterite surface after being treated with (a) deionized water, (b) CHA, (c) both Pb(II) and CHA

In Fig. 10(a), the cassiterite surface treated solely with lead ions exhibits characteristic peaks with a binding energy of 143.36 eV for Pb 4f<sub>5/2</sub> and 138.54 eV for Pb 4f<sub>7/2</sub>. These peaks are likely attributed to lead hydroxides, consistent with previous literature findings (Nie et al., 2023). This result confirms the adsorption of lead ions onto the cassiterite surface. Fig. 10(b) presents the XPS spectrum of the cassiterite surface treated with CHA following lead ion modification. It can be observed that the binding energy of Pb 4f<sub>5/2</sub> is shifted to 143.58 eV in the direction of higher binding energy, while the binding energy of Pb 4f<sub>7/2</sub> is also shifted to 138.78 eV in the direction of higher binding energy. These shifts correspond to an increase of 0.22 eV and 0.24 eV, respectively. This finding indicates that when the cassiterite surface is adsorbed by lead ions, it provides additional sites for CHA adsorption on the cassiterite surface. According to the above experimental results, a diagram of the adsorption model of CHA on the cassiterite surface under lead ion activation conditions was depicted as shown in Fig. 11.

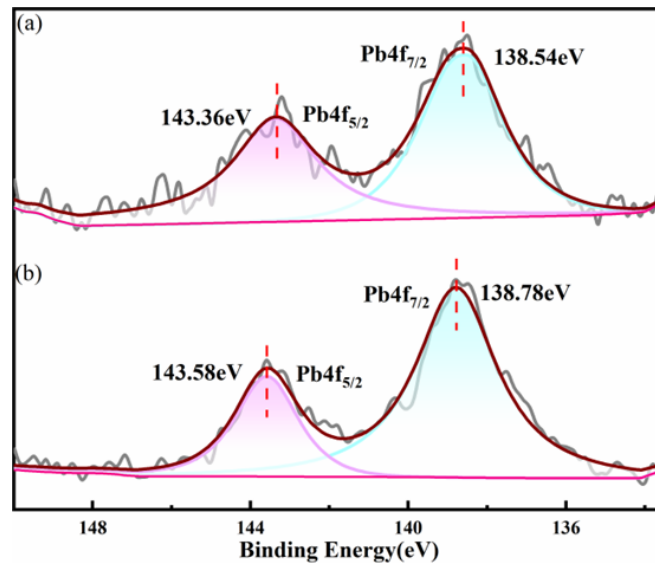


Fig. 10. XPS narrow-scan spectra of Pb4f on the cassiterite surface after being treated with (a) Pb(II), (b) Pb(II) and CHA

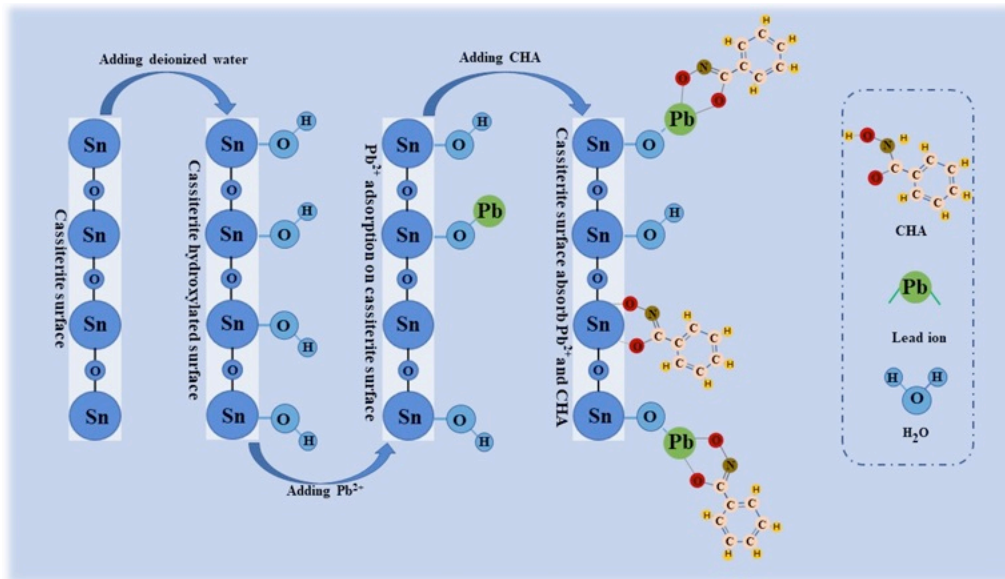


Fig.11. Schematic diagram of lead ion-activated cassiterite surface promoting CHA adsorption model

#### 4. Conclusions

Comparative and mechanistic studies were conducted to investigate the flotation performance of cassiterite using BHA and CHA as collectors under the activation conditions of  $Pb^{2+}$  ions, through microflotation experiments. The adsorption mechanism of CHA on the cassiterite surface, both in the presence and absence of  $Pb^{2+}$  ions, was examined through experiments involving adsorption measurements, infrared spectral analysis, and XPS analysis. The following conclusions can be drawn from the study's results:

- (i) The results of the flotation experiments demonstrate that within the pH range of 4 to 12, CHA exhibits a stronger ability to adsorb cassiterite in comparison to BHA. The optimal flotation pH conditions were determined to be between 9 and 10. Under these conditions, using CHA as the flotation collector, cassiterite achieved a flotation recovery of 92.53%, while BHA only achieved a recovery of 75%.
- (ii) The results of the adsorption tests indicated that the adsorption of both CHA and BHA on the cassiterite surface increased with the increase in the amount of the collectors, consistent with the results from the flotation experiments regarding the concentration of the flotation collectors.

Furthermore, the adsorption quantity of CHA on the cassiterite surface was significantly higher than that of BHA.

- (iii) XPS results directly confirm that the terminal hydroxyl oxygen atom on the cassiterite surface serves as the primary reaction site for the adsorption of  $Pb^{2+}$  ions. The Pb atoms adsorbed on the cassiterite surface act as the main active sites for subsequent interaction with the BHA capturing agent. In the presence of the  $Pb^{2+}$  ion activator,  $Pb^{2+}$  ions first react with the terminal hydroxyl oxygen atoms on the surface of cassiterite, followed by BHA's reaction with the iron atoms adsorbed on the cassiterite surface to form Pb-BHA complexes.

### Acknowledgements

This work was financially supported by the National Natural Science Foundation of China (No. 51674291).

### References

- ANGADI, S., SREENIVAS, T., JEON, H.-S., BAEK, S.-H., MISHRA, B., 2015. *A review of cassiterite beneficiation fundamentals and plant practices*. Minerals. Engineering, 70, 178-200.
- CAO, Y., XIE, X., TONG, X., FENG, D., LV, J., CHEN, Y., SONG, Q., 2021. *The activation mechanism of Fe (II) ion-modified cassiterite surface to promote salicylhydroxamic acid adsorption*. Miner. Eng., 160, 106707.
- FENG, Q., WEN, S., CAO, Q., DENG, J., ZHAO, W., 2016. *The effect of chloride ions on the activity of cerussite surfaces*. Minerals., 6(3), 92.
- FENG, Q., WEN, S., ZHAO, W., CHEN, Y., 2018. *Effect of calcium ions on adsorption of sodium oleate onto cassiterite and quartz surfaces and implications for their flotation separation*. Sep. Purif. Technol., 200, 300-306.
- FENG, Q., ZHAO, W., WEN, S., CAO, Q., 2017. *Activation mechanism of lead ions in cassiterite flotation with salicylhydroxamic acid as collector*. Sep. Purif. Technol., 178, 193-199.
- GRUNER, H., BILSING, U., 1992. *Cassiterite flotation using styrene phosphonic acid to produce high-grade concentrates at high recoveries from finely disseminated ores-comparison with other collectors and discussion of effective circuit configurations*. Miner. Eng., 5(3-5), 429-434.
- HUANG, J., ZHONG, H., QIU, X., WANG, S., ZHAO, G., GAO, Y., DAI, Z., LIU, G., 2013. *Flotation behavior and adsorption mechanism of cyclohexyl hydroxamic acid to wolframite*. Chin. J. Nonferr. Met, 23, 2023-2030.
- JIN, S., OU, L., 2022. *Comparison of the Effects of Sodium Oleate and Benzohydroxamic Acid on Fine Scheelite and Cassiterite Hydrophobic Flocculation*. Minerals, 12(6), 687.
- JIN, S., ZHANG, P., OU, L., ZHANG, Y., CHEN, J., 2021. *Flotation of cassiterite using alkyl hydroxamates with different carbon chain lengths: A theoretical and experimental study*. Miner. Eng., 170, 107025.
- CHEN, J.H., 2021. *The interaction of flotation reagents with metal ions in mineral surfaces: A perspective from coordination chemistry*. Minerals Engineering., 171: 107067
- CHEN, J.H., LI, Y.Q., 2022. *Orbital symmetry matching study on the interactions of flotation reagents with mineral surfaces*. Minerals Engineering., 179: 107469
- LEISTNER, T., EMBRECHTS, M., LEISTNER, T., CHELGANI, S.C., OSBAHR, I., MÖCKEL, R., PEUKER, U., RUDOLPH, M., 2016. *A study of the reprocessing of fine and ultrafine cassiterite from gravity tailing residues by using various flotation techniques*. Miner. Eng., 96, 94-98.
- LI, F., ZHONG, H., ZHAO, G., WANG, S., LIU, G., 2015. *Flotation performances and adsorption mechanism of  $\alpha$ -hydroxyoctyl phosphinic acid to cassiterite*. Appl. Surf. Sci., 353, 856-864.
- MACHESKY, M., WESOŁOWSKI, D., ROSENQVIST, J.R., PREDOTA, M., VLCEK, L., RIDLEY, M., KOHLI, V., ZHANG, Z., FENTER, P., CUMMINGS, P., 2011. *Comparison of cation adsorption by isostructural rutile and cassiterite*. Langmuir., 27(8), 4585-4593.
- NIE, S., GUO, Z., TIAN, M., SUN, W., 2023. *Selective flotation separation of cassiterite and calcite through using cinnamohydroxamic acid as the collector and  $Pb^{2+}$  as the activator*. Colloids and Surfaces A: Physicochemical and Engineering Aspects., 666, 131262.
- OCELLI, M., STENCEL, J., 1987. *X-ray photoelectron spectroscopy (XPS) characterization of dual function cracking catalysts (DFCC) mixtures*. American Chemical Society, Division of Petroleum Chemistry, Preprints(USA), 32(CONF-8708311-).
- PANDEY, S., MISHRA, K.K., GHOSH, P., SINGH, A.K., JHA, S.K., 2023. *Characterization of tin-plated steel*. Frontiers in Materials., 10, 1113438.

- QIN, W.-Q., REN, L.-Y., XU, Y.-B., WANG, P.-P., MA, X.-H., 2012. *Adsorption mechanism of mixed salicylhydroxamic acid and tributyl phosphate collectors in fine cassiterite electro-flotation system*. Journal of Central South University., 19(6), 1711-1717.
- QIN, W., XU, Y., LIU, H., REN, L., YANG, C., 2011. *Flotation and surface behavior of cassiterite with salicylhydroxamic acid*. Ind. Eng. Chem. Res., 50(18), 10778-10783.
- RUAN, Y., ZHANG, Z., LUO, H., XIAO, C., ZHOU, F., CHI, R., 2018. *Effects of metal ions on the flotation of apatite, dolomite and quartz*. Minerals, 8(4), 141.
- SARVARAMINI, A., LARACHI, F., HART, B., 2016. *Collector attachment to lead-activated sphalerite—Experiments and DFT study on pH and solvent effects*. Appl. Surf. Sci., 367, 459-472.
- SCHNEIDER, M., LANGKLOTZ, U., KÖRSTEN, O., GIERTH, U., 2023. *Passive layer investigation on tin and tin solder alloys*. Mater. Corros.,
- SUKUNTA, J., WISITSORAAT, A., TUANTRANONT, A., PHANICHPHANT, S., LIEWHIRAN, C., 2017. *Highly-sensitive H<sub>2</sub>S sensors based on flame-made V-substituted SnO<sub>2</sub> sensing films*. Sensors and Actuators B: Chemical, 242, 1095-1107.
- SUN, Q., LU, Y., WANG, S., ZHONG, H., 2020. *A novel surfactant 2-(benzylthio)-acetohydroxamic acid: Synthesis, flotation performance and adsorption mechanism to cassiterite, calcite and quartz*. Appl. Surf. Sci., 522, 146509.
- TIAN, M., GAO, Z., HAN, H., SUN, W., HU, Y., 2017. *Improved flotation separation of cassiterite from calcite using a mixture of lead (II) ion/benzohydroxamic acid as collector and carboxymethyl cellulose as depressant*. Miner. Eng., 113, 68-70.
- TIAN, M., LIU, R., GAO, Z., CHEN, P., HAN, H., WANG, L., ZHANG, C., SUN, W., HU, Y., 2018. *Activation mechanism of Fe (III) ions in cassiterite flotation with benzohydroxamic acid collector*. Miner. Eng., 119, 31-37.
- WANG, P.-P., QIN, W.-Q., REN, L.-Y., QIAN, W., LIU, R.-Z., YANG, C.-R., ZHONG, S.-P., 2013. *Solution chemistry and utilization of alkyl hydroxamic acid in flotation of fine cassiterite*. Transactions of Nonferrous Metals Society of China., 23(6), 1789-1796.
- WU, X., ZHU, J., 2016. *Selective flotation of cassiterite with benzohydroxamic acid*. Miner. Eng., 19(14), 1410-1417.
- XIE, R., ZHU, Y., LIU, J., LI, Y., 2021. *Effects of metal ions on the flotation separation of spodumene from feldspar and quartz*. Miner. Eng., 168, 106931.
- XU, Y., QIN, W., 2014. *Surface analysis of cassiterite with sodium oleate in aqueous solution*. Sep. Sci. Technol., 47(3), 502-506.
- ZHAO, G., WANG, S., ZHONG, H., 2015. *Study on the activation of scheelite and wolframite by lead nitrate*. Minerals., 5(2), 247-258.
- ZHAO, G., ZHONG, H., QIU, X., WANG, S., GAO, Y., DAI, Z., HUANG, J., LIU, G., 2013. *The DFT study of cyclohexyl hydroxamic acid as a collector in scheelite flotation*. Miner. Eng., 49, 54-60.
- ZHOU, Y., TONG, X., SONG, S., WANG, X., DENG, Z., XIE, X., 2014. *Beneficiation of cassiterite fines from a tin tailing slime by froth flotation*. Sep. Sci. Technol., 49(3), 458-463.
- ZHU, L., LIU, J., ZHU, Y., GONG, G., HAN, Y., 2022. *Mechanism of HCA and CEPPA in flotation separation of cassiterite and fluorite*. Miner. Eng., 187, 107773.